Effect of quantum fluctuation in error-correcting codes

Yosuke Otsubo
Graduate School of Frontier Sciences, The University of Tokyo, Kashiwa, Chiba 277-5861, Japan

Jun-ichi Inoue
Complex Systems Engineering, Graduate School of Engineering, Hokkaido University, Sapporo, Hokkaido 060-8628, Japan

Kenji Nagata
Graduate School of Frontier Sciences, The University of Tokyo, Kashiwa, Chiba 277-5861, Japan

Masato Okada*
Graduate School of Frontier Sciences, The University of Tokyo, Kashiwa, Chiba 277-5861, Japan and Brain Science Institute, RIKEN, Wako, Saitama 351-0198, Japan

(Received 2 April 2012; published 30 November 2012)

We discuss the decoding performance of error-correcting codes based on a model in which quantum fluctuations are introduced by means of a transverse field. The essential issue in this paper is whether quantum fluctuations improve the decoding quality compared with the conventional estimation based on thermal fluctuations, which is called finite-temperature decoding. We found that an estimation incorporating quantum fluctuations approaches the optimal performance of finite-temperature decoding. The results are illustrated by numerically solving saddle-point equations and performing a Monte Carlo simulation. We also evaluated the upper bound of the overlap between the original sequence and the decoded sequence derived from the equations of state for the order parameters, which is a measure of the decoding performance.

DOI: 10.1103/PhysRevE.86.051138 PACS number(s): 02.50.−r, 75.10.Nr, 05.50.+q, 89.70.−a

I. INTRODUCTION

Problems in information processing have recently been investigated in terms of a mean-field spin glass model. For example, problems dealing with image restoration, error-correcting codes, neural networks, and optimization can be represented as a mean-field spin glass model, and their information processing quality levels have been investigated from a statistical mechanical viewpoint [1–4]. In particular, Sourlas has represented error-correcting codes in terms of a mean-field spin glass model that can be considered as a generalization of the Mattis model [2,5]. Rujan suggested that the decoding procedure of the model can be modified so it operates not in the ground state but in a state at a finite temperature [6]. The decoding of other error-correcting codes, e.g., the low-density parity check code and the convolutional code, has also been investigated by means of statistical-mechanical analysis [7,8].

Quantum spin glass models have been investigated since the 1980s in order to clarify the microscopic properties of spin glasses. A well-known problem is how the transverse field, which induces the tunneling effect between states, affects the quantum phase transition [9]. The properties of the Sherrington-Kirkpatrick model with a transverse field have been investigated by using the mean-field approximation and the replica method, and it has been found that there is a phase transition from the spin glass phase to the paramagnetic phase depending on the strength of the transverse field [10,11]. The replica method has also been used to investigate the random energy model [12]. Moreover, the replica symmetry breaking solution when quantum effects are taken into account has been researched [13,14].

Although there have been numerous studies on information processing using classical spin glasses as a model and on the properties of quantum spin glasses themselves, the effect of introducing a transverse field, i.e., quantum fluctuation, into an information processing model has not been thoroughly investigated. We expected that quantum fluctuations would induce some changes in decoding quality compared with classical decoding, as inspired by the annealing method. The quantum annealing is an algorithm for finding the global minimum of an objective function for a process analogous to simulated annealing by using quantum fluctuation, and that is known to be a useful method in the optimization problems [15,16]. Inoue has investigated the topic of image restoration by using quantum fluctuations, but that problem corresponds not to a spin glass model, which has random interactions among spins, but to a random field model [17].

In this paper, we focus on the SOURLAS code, an error-correcting code that can be described in terms of a mean-field spin glass model. We investigate the decoding performance of the SOURLAS code on the basis of a model in which a quantum fluctuation is introduced by means of the transverse field.

This paper is organized as follows. In Sec. II, we present a Bayes formulation of the SOURLAS code. In Sec. III, we pose an open question and state the goal of this paper. In Sec. IV, we analyze the model. In Sec. V, we present analytical and simulation results and evaluate the upper bound of the overlap, which is a measure of the decoding performance of the SOURLAS code. Section VI contains a summary and discussion of the results.

*okada@mns.k.u-tokyo.ac.jp

II. ERROR-CORRECTING CODES AND QUANTUM SPIN GLASS MODEL

First, we describe the error-correcting code model and *the maximum a posteriori probability* (MAP) and *the maximizer of the posterior marginals* (MPM) estimates. Next, we extend the model to one with a quantum transverse field, i.e., with quantum fluctuations.

The idea of error-correcting codes is to add redundancy to messages so that receivers can recover the original message from noisy output. Suppose that the original message is represented by a configuration of Ising spins $\boldsymbol{\xi} = \{\xi_1, \ldots, \xi_N\}$ $(\xi_i = \pm 1, i = 1, \ldots, N)$ that has been generated according to a probability distribution function $P(\boldsymbol{\xi})$. We can formulate the SOURLAS code as a mean-field model with p-body spin interactions [2]. We assume that the sender transmits all possible combinations ${}_N C_p$ of the products of p-components in an N-dimensional vector $\boldsymbol{\xi}$ with components $\xi_{i1}, \ldots, \xi_{ip}$ through a Gaussian channel with mean $J_0 p! \xi_{i1}, \ldots, \xi_{ip}/N^{p-1}$ and variance $J^2 p!/2N^{p-1}$. That is, the output probability is given by

$$\begin{aligned} &P(J_{i1,\ldots,ip}|\xi_{i1}, \ldots, \xi_{ip}) \\ &= \left(\frac{N^{p-1}}{J^2 \pi p!}\right)^{\frac{1}{2}} \exp\left\{-\frac{N^{p-1}}{J^2 p!}\left(J_{i1,\ldots,ip} - \frac{J_0 p! \xi_{i1}, \ldots, \xi_{ip}}{N^{p-1}}\right)^2\right\}, \end{aligned} \quad (1)$$

where J and J_0 are independent of N and p, and J_0/J denotes the signal-to-noise ratio. The expression $P(J_{i1,\ldots,ip}|\xi_{i1}, \ldots, \xi_{ip})$ denotes the conditional probability of the signal $J_{i1,\ldots,ip}$ given the encoded message $\xi_{i1}, \ldots, \xi_{ip}$. Furthermore, we assume that each bit ξ_i in the original message $\boldsymbol{\xi}$ is generated independently (the so-called memoryless channel), i.e.,

$$P(\boldsymbol{J}|\boldsymbol{\xi}) = \prod_{i=1}^{N} P(J_{i1,\ldots,ip}|\xi_{i1}, \ldots, \xi_{ip}), \quad (2)$$

and the prior probability of the message is uniform, i.e., $P(\xi) = 2^N$.

We can express the posterior probability $P(\boldsymbol{\sigma}|\boldsymbol{J})$ in terms of Eqs. (1) and (2) by using the Bayes formula,

$$\begin{aligned} P(\boldsymbol{\sigma}|\boldsymbol{J}) &= \frac{P(\boldsymbol{J}|\boldsymbol{\sigma})P(\boldsymbol{\sigma})}{\mathrm{Tr}_{\boldsymbol{\sigma}} P(\boldsymbol{J}|\boldsymbol{\sigma})P(\boldsymbol{\sigma})} & (3) \\ &\propto \exp\left(\beta \sum_{i1<\cdots<ip} J_{i1,\ldots,ip}\sigma_{i1}, \ldots, \sigma_{ip}\right), & (4) \end{aligned}$$

where β $(\equiv 1/T)$ is the controlled parameter in the signal retrieval algorithm. The optimal retrieval can be achieved if a β corresponding to the noise level is chosen as $2J_0/J^2$ in the Gaussian channel (1) [25].

We shall write the dynamical variables used for decoding as $\boldsymbol{\sigma} = \{\sigma_1, \ldots, \sigma_N\}$ $(\sigma_i = \pm 1, i = 1, \ldots, N)$. Equation (4) represents the probability distribution of the inferred spin configuration $\boldsymbol{\sigma}$ given the output $\boldsymbol{J}$. We can regard the right-hand side of Eq. (4) as being a Gibbs-Boltzmann distribution, and hence we shall call β the inverse temperature.

We might choose the spin configuration that maximizes Eq. (4) as the decoded sequence. This is the MAP estimate corresponding to finding the ground state of the following Hamiltonian:

$$H = -\sum_{i1<\cdots<ip} J_{i1,\ldots,ip}\sigma_{i1}, \ldots, \sigma_{ip}. \quad (5)$$

The sum in this Hamiltonian runs over all possible combinations of p spins out of N spins. Therefore, we can see that the problem of the error-correcting code model is closely related to a ground-state search in the mean-field models of spin glasses, e.g., the SK model $(p = 2)$ and the random energy model $(p \to \infty)$ [18,19].

In the MPM estimate framework, we focus on a single bit σ_i and consider the posterior marginal probability:

$$P(\sigma_i|\boldsymbol{J}) = \frac{\mathrm{Tr}_{\boldsymbol{\sigma}(\neq\sigma_i)} \exp\left(\beta \sum_{i1<\cdots<ip} J_{i1,\ldots,ip}\sigma_{i1}, \ldots, \sigma_{ip}\right)}{\mathrm{Tr}_{\boldsymbol{\sigma}} \exp\left(\beta \sum_{i1<\cdots<ip} J_{i1,\ldots,ip}\sigma_{i1}, \ldots, \sigma_{ip}\right)}. \quad (6)$$

Let us compare $P(\sigma_i = +1|\boldsymbol{J})$ and $P(\sigma_i = -1|\boldsymbol{J})$. The inferred spin in terms of the MPM estimate is given by

$$\begin{aligned} \hat{\xi}_i &= \mathrm{sgn}[P(\sigma_i = +1|\boldsymbol{J}) - P(\sigma_i = -1|\boldsymbol{J})] \\ &= \mathrm{sgn}\big(\mathrm{Tr}_{\sigma_i}\sigma_i P(\sigma_i|\boldsymbol{J})\big) = \mathrm{sgn}\left(\frac{\mathrm{Tr}_{\boldsymbol{\sigma}}\sigma_i e^{-\beta H}}{\mathrm{Tr}_{\boldsymbol{\sigma}} e^{-\beta H}}\right) \equiv \mathrm{sgn}\langle\sigma_i\rangle_\beta, \end{aligned} \quad (7)$$

where we have defined the brackets $\langle\cdot\rangle_\beta$ as

$$\langle\cdot\rangle_\beta = \frac{\mathrm{Tr}_{\boldsymbol{\sigma}}(\cdot)e^{-\beta H}}{\mathrm{Tr}_{\boldsymbol{\sigma}} e^{-\beta H}}. \quad (8)$$

Equation (7) means calculating the local magnetization at a finite temperature T $(\equiv 1/\beta)$. Hence, the MPM estimate is also called *finite-temperature decoding*.

Now, let us introduce the overlap M, defined as

$$\begin{aligned} M^{\mathrm{classic}}(\beta) &= \mathrm{Tr}_{\boldsymbol{\xi}} \int \prod_{i1<\cdots<ip} dJ_{i1,\ldots,ip} P(\boldsymbol{J}|\boldsymbol{\xi})P(\boldsymbol{\xi})\xi_i \mathrm{sgn}\langle\sigma_i\rangle_\beta & (9) \\ &\equiv [\xi_i \mathrm{sgn}\langle\sigma_i\rangle_\beta], & (10) \end{aligned}$$

which is the quality of the retrieved signal. Henceforth, we use the bracket $[\cdot]$ for the data average over the distribution $P(\boldsymbol{J}|\boldsymbol{\xi})P(\boldsymbol{\xi})$ as in Eq. (9). The larger the overlap is, the better the decoding performance will be. It is known that the MPM estimate is better than the MAP estimate, i.e., ground-state decoding, if we choose the temperature appropriately [6,20]. This temperature is well known as the *Nishimori temperature*, which is $\beta = 2J_0/J^2 \equiv \beta_p$ for Eqs. (1) and (4).

We can extend the above formulation to the quantum case by adding a *quantum transverse field* term leading to the tunnel effect,

$$\hat{H}_1 \equiv -\Gamma \sum_i \hat{\sigma}_i^x, \quad (11)$$

to the Hamiltonian (5) as a *quantum fluctuation*. The expression $\hat{\sigma}_i^x$ denotes the x component of the Pauli matrix, and Γ controls the quantum fluctuation strength. Thus, a quantum Hamiltonian can be obtained by adding a transverse field (11) to the classical Hamiltonian (5):

$$\hat{H} = -\sum_{i1<\cdots<ip} J_{i1,\ldots,ip}\hat{\sigma}_{i1}^z, \ldots, \hat{\sigma}_{ip}^z - \Gamma \sum_i \hat{\sigma}_i^x \equiv \hat{H}_0 + \hat{H}_1, \quad (12)$$

where $\hat{\sigma}_i^z$ is the z component of the Pauli matrix. In the case of $\Gamma = 0$, the system corresponds to a classical system without any quantum effects. To understand the effect of this quantum fluctuation [Eq. (11)], let us consider the case of a single-spin system. Denoting the eigenstates of $\hat{\sigma}^z$ as $|+\rangle = (1,0)^t$ and $|-\rangle = (0,1)^t$, the x component of the Pauli matrix becomes $\hat{\sigma}^x = |+\rangle\langle-| + |-\rangle\langle+|$. Thus, we find that $\hat{\sigma}^x|\pm\rangle = |\mp\rangle$, that is, the up-state described by $|+\rangle$ transits to the down-state described by $|-\rangle$ by means of the tunnel effect.

The overlap in the case of a quantum system (12) is defined as

$$M(\beta,\Gamma) = \operatorname*{Tr}_{\boldsymbol{\xi}} \int \prod_{i1<\cdots<ip} dJ_{i1,\ldots,ip} P(\boldsymbol{J}|\boldsymbol{\xi}) P(\boldsymbol{\xi}) \xi_i \operatorname{sgn}\langle\hat{\sigma}_i^z\rangle_{\beta,\Gamma}$$
$$= [\xi_i \operatorname{sgn}\langle\hat{\sigma}_i^z\rangle_{\beta,\Gamma}]. \tag{13}$$

The inferred spin in terms of the MPM estimate including a quantum fluctuation corresponding to Eq. (7) is written as a density matrix: $\hat{\rho} \equiv e^{-\beta\hat{H}(\sigma|\boldsymbol{J})}/\mathrm{Tr}e^{-\beta\hat{H}(\sigma|\boldsymbol{J})}$ [21]:

$$\hat{\xi}_i = \operatorname{sgn}[\mathrm{Tr}(\hat{\sigma}_i^z\hat{\rho})]. \tag{14}$$

III. OPEN QUESTION

Figure 1 sketches the solution presented in this paper. First, we describe a system without quantum fluctuations. We use a MAP estimate to infer the ground state corresponding to the state with $T = 0$. After that, we consider the case of finite-temperature decoding in a model without a quantum fluctuation. The corresponding MPM estimate clearly gives a different result from the MAP estimate, and it results in optimal decoding at the Nishimori temperature [6,20]. This means the overlap M is at a maximum at the optimal temperature (see the left panel in Fig. 1). Thus, in the case of the SOURLAS code, it is important to control the temperature of decoding. We call such an estimate without considering quantum fluctuations a thermal MPM estimate.

However, it is still unclear how quantum fluctuations affect the decoding performance of error-correcting codes represented as mean-field spin glass models. It is well known that the annealing method can use quantum fluctuations to find the lowest energy state, i.e., the ground state, instead of thermal ones [15,22]. This annealing method is called *quantum annealing* (QA), in contrast to *simulated annealing* (SA) using thermal fluctuations. In this context, quantum fluctuations behave similarly to thermal fluctuations. Here, we shall focus on the decoding performance in the Γ/J-T/J space in Fig. 1 and investigate whether a maximum overlap exists and whether it is more maximal than the classical one given by the thermal MPM estimate. That is, the problem is to clarify the decoding performance of the MPM estimate based on quantum fluctuations (the right panel in Fig. 1). The key point of the MPM estimate incorporating quantum fluctuations is making an appropriate ensemble according to the noise of a Gaussian channel by using not only thermal fluctuation but also quantum fluctuation.

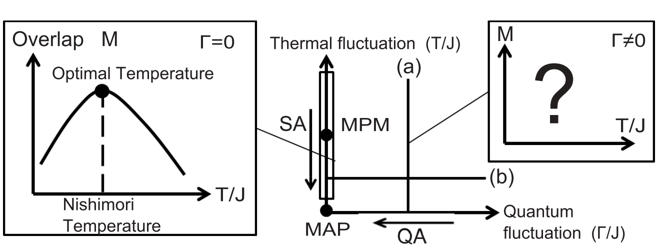

FIG. 1. Sketch of this paper. Quantum annealing (QA) and simulated annealing (SA) are methods for finding the ground state.

To address this, we find a way to express the overlap as a function of the macroscopic parameters by using the standard replica and saddle-point methods. The results obtained by these analytical approaches and by numerical experiments using the Monte Carlo method are then presented, and an inequality is derived to establish an upper bound of the overlap for the quantum fluctuations.

IV. ANALYSIS OF THE MEAN-FIELD MODEL

To explicitly calculate the decoding performance of the error-correcting code model with quantum fluctuations, we use the standard replica method to express the overlap equation [Eq. (13)] from the saddle-point equations that determine the equilibrium state.

First, we apply a *Suzuki-Trotter* (ST) *decomposition* [23],

$$\exp(\hat{K} + \hat{U}) = \lim_{P\to\infty} (e^{\hat{K}/P} e^{\hat{U}/P})^P, \tag{15}$$

to the partition function $Z = \mathrm{Tr}\exp(-\beta\hat{H})$ with $\hat{U} = -\sum J_{i1,\ldots,ip}\hat{\sigma}_{i1}^z,\ldots,\hat{\sigma}_{ip}^z$, $\hat{K} = -\Gamma\sum_i \hat{\sigma}_i^x$ in order to cast the problem as an equivalent classical spin system. Accordingly, Z and the effective Hamiltonian H_{eff} are given by

$$Z = \lim_{P\to\infty} \left(\frac{1}{2}\sinh\frac{2\beta\Gamma}{P}\right)^{\frac{NP}{2}} \mathrm{Tr}_{\boldsymbol{\sigma}} \exp(-H_{\text{eff}}), \tag{16}$$

$$H_{\text{eff}} = \frac{\beta}{P}\sum_{t=1}^{P}\sum_{i_1<\cdots<i_p} J_{i_1,\ldots,i_p}\sigma_{i1}(t),\ldots,\sigma_{ip}(t)$$
$$+ \frac{1}{2}\log\left(\coth\frac{\beta\Gamma}{P}\right)\sum_{i=1}^{N}\sum_{t=1}^{P}\sigma_i(t)\sigma_i(t+1), \tag{17}$$

where P is called the Trotter number and t is the Trotter index. We can see that the dimensionality of the corresponding classical system after application of the ST formula increases by 1. Using the well-known replica method [18],

$$[\log\ Z] = \lim_{n\to 0}\frac{[Z^n] - 1}{n}, \tag{18}$$

we calculate the free energy density $[\log Z]$ in terms of $[Z^n]$. The subsequent application of a gauge transformation $J_{i1,\ldots,ip} \to J_{i1,\ldots,ip}\xi_{i1},\ldots,\xi_{ip}$ and $\sigma_i \to \sigma_i\xi_i$ in $[Z^n]$ removes $\boldsymbol{\xi}$ from the integrand of the SOURLAS code model. Thus, the problem turns out to be equivalent to the case of $\xi_i = 1(\forall i)$, i.e., the ferromagnetic gauge. Hence, in the thermodynamic limit $N \to \infty$, we can obtain the saddle-point equations with respect to the order parameters [21,24]:

$$[\langle\sigma_i^\mu(t)\rangle_{\beta,\Gamma}] \equiv m = \int Dw \int Dz \frac{\Phi\sinh\Xi}{\Omega\Xi}, \tag{19}$$

$$[\langle\sigma_i^\mu(t)\sigma_i^\nu(t')\rangle_{\beta,\Gamma}] \equiv q = \int Dw \left(\int Dz\frac{\Phi\sinh\Xi}{\Omega\Xi}\right)^2, \tag{20}$$

$$[\langle\sigma_i^\mu(t)\sigma_i^\mu(t')\rangle_{\beta,\Gamma}] \equiv \chi = \int \frac{Dw}{\Omega}\int Dz\left(\frac{\beta^2\Gamma^2\sinh\Xi}{\Xi^3}+\frac{\Phi^2\cosh\Xi}{\Xi^2}\right), \tag{21}$$

$$\Xi = \sqrt{\Phi^2+\beta^2\Gamma^2}, \tag{22}$$

$$\phi \equiv \frac{\Phi}{\beta} = pJ_0m^{p-1} + wJ\sqrt{\frac{pq^{p-1}}{2}} + zJ\sqrt{\frac{p(\chi^{p-1}-q^{p-1})}{2}}, \tag{23}$$

$$\Omega \equiv \int Dz\cosh\Xi. \tag{24}$$

Here, μ and ν mean the replica indices and $\int Du(\cdot) = \int_{-\infty}^{\infty} du(\cdot)e^{-\frac{u^2}{2}}/\sqrt{2\pi}$. Note that the above equations of state for the order parameters (19)–(24) are obtained under replica symmetry and the static approximation [25].

The final goal in this section is to derive the expression of the overlap M. The overlap in the quantum case can be obtained in a similar way as is done in the classical system [26]. The physical meanings of m and q are the magnetization and the spin glass order parameter, respectively, and each parameter can be denoted as $m = [\langle\sigma_i\rangle_{\beta,\Gamma}]$, $q = [\langle\sigma_i\rangle^2_{\beta,\Gamma}]$. By comparing these expressions and Eqs. (19) and (20), we see that $\int Dz\frac{\Phi\sinh\Xi}{\Omega\Xi}$ is closely related to $\langle\sigma_i\rangle_{\beta,\Gamma}$. We can confirm this by adding $h\sum_i \sigma_i^\mu(t)\sigma_i^\nu(t')$ to $[Z^n]$. The detailed calculations are given in Appendix A. The final form of the overlap $M(\beta,\Gamma)$ is

$$M(\beta,\Gamma) = \int Dw\,\mathrm{sgn}\left(\int Dz\frac{\Phi\sinh\Xi}{\Omega\Xi}\right). \tag{25}$$

In the case of a classical system, i.e., $\Gamma = 0$, the overlap M^{classic} can be derived from Eq. (25) for $\int Dz\frac{\Phi\sinh\Xi}{\Omega\Xi} = \tanh\beta(wJ\sqrt{\frac{pq^{p-1}}{2}}+pJ_0m^{p-1})$ as

$$M^{\mathrm{classic}}(\beta) = \int Dw\,\mathrm{sgn}\left(wJ\sqrt{\frac{pq^{p-1}}{2}}+pJ_0m^{p-1}\right). \tag{26}$$

This form is the same one derived from the previous work [20].

V. RESULTS

Below, we numerically solve Eqs. (19)–(25) and discuss the performance of decoding based on a model with quantum fluctuations. We also show the results of a quantum Monte Carlo simulation and calculate an upper bound of the overlap.

A. Stability of error correction

As a preliminary step to calculating the decoding performance, we shall determine whether decoding is possible by solving Eqs. (19)–(24). As we increase the strength of the transverse field Γ/J, i.e., the quantum fluctuation, we observe a first-order transition at a finite Γ/J for $p = 3$, $T/J = 0.1$, and $J_0/J = 1.0$ [see Fig. 2(a)]. In the ferromagnetic phase (ferro: $m > 0, q > 0, \chi > 0$), the overlap M has a finite value, which means that error correction is possible. On the other hand, the paramagnetic phase (para: $m = 0$, $q = 0$, $\chi > 0$) is a random guess phase for which error correction is impossible.

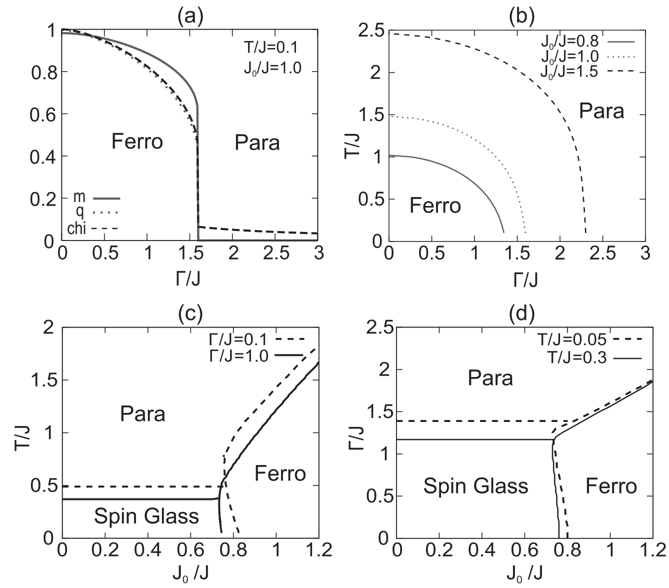

FIG. 2. (a) Dependence of the order parameters m, q, and χ on the level of quantum fluctuation Γ/J for $p = 3$, $T/J = 0.1$, and $J_0/J = 1.0$. (b)–(d) Phase diagram for each parameter with $p = 3$.

The phase diagrams of the model are shown in Figs. 2(b)–2(d). As the signal-to-noise (SN) ratio J_0/J increases, the ferromagnetic phase becomes larger. We can see that the ferromagnetic phase exists in the low-temperature region $T \sim 0$. Moreover, the ferromagnetic phase disappears, and then the nonretrieval spin glass phase (spin glass: $m = 0$, $q > 0$, $\chi > 0$) appears in its place as the SN ratio J_0/J decreases. Note that the phase boundary in the low-temperature limit ($T \to 0$) has not been determined.

B. Decoding performance

Now let us investigate the decoding performance in the ferromagnetic phase by calculating the overlap M analytically and in Monte Carlo simulations.

1. *Analytical results*

First, we numerically solved Eqs. (19)–(25) and plotted the dependence of the overlap M on T/J for $p = 3$ and $J_0/J = 1.0$. Figure 3(a) shows that the optimal amplitude of temperature T/J at $\Gamma/J = 0.0$ is 0.5, which corresponds to the Nishimori temperature in the case of $J_0/J = 1.0$. The overlap for $\Gamma/J = 0.3$ is at a maximum for a finite T/J smaller than 0.5. The maximum value of M is approximately 0.983, which is equal to the case of $\Gamma = 0.0$. Thus, the MPM estimate with a quantum fluctuation seems to achieve the same optimal decoding performance as the thermal MPM estimate. Next, let us consider a large quantum fluctuation, $\Gamma/J = 0.8$. In this case, the overlap M decreases monotonically as the temperature T/J increases. In the low-temperature region, however, we find that the overlap due to the quantum fluctuation is larger than in the classical case. This means that the quantum fluctuations do make the decoding performance

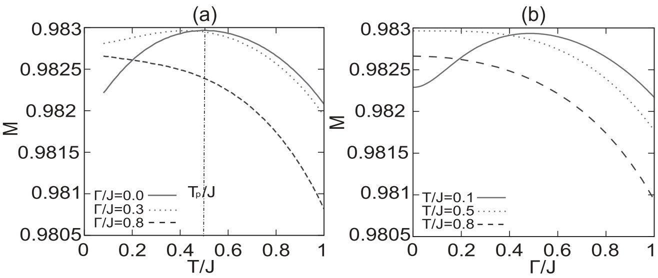

FIG. 3. (a) Dependence of the overlap M on temperature T/J for $p=3$ and $J_0/J=1.0$, where Γ/J is fixed to 0.0, 0.3, and 0.8. (b) Dependence of M on the level of quantum fluctuation Γ/J for $p=3$ and $J_0/J=1.0$, where T/J is fixed to 0.1, 0.5, and 0.8. In these cases, the Nishimori temperature corresponds to 0.5. These results correspond to lines (a) and (b) in Fig. 1, respectively.

better than a classical estimate based on the thermal fluctuation when the temperature is lower than the Nishimori temperature.

Figure 3(b) shows the dependence of the overlap M on Γ/J. At low temperature, $T/J=0.1$, there is a quantum fluctuation that maximizes the overlap at the finite amplitude of Γ/J. The maximum overlap is approximately 0.983, which is equal to the value in the classical case. We see that the overlap in the case of $T/J=0.5$, which corresponds to the Nishimori temperature, reaches a maximum at $\Gamma=0.0$. The overlap has a lower value in the case of $T/J=0.8$.

Figure 4 shows the overlap for $p=2$ and 4. These overlaps are qualitatively similar to those in Fig. 3. We also find that the overlap is large if the number of spin interactions p is large. In the case of the random energy model, $p\to\infty$, we can use Eqs. (19)–(24) to prove that $M\to 1$ for $\chi\sim q\sim 1, m\sim 1$ [24].

Figure 5 shows the phase diagram for the overlap in T/J-Γ/J space. The gradation indicates the amount of the overlap, and the solid line represents the maximum overlap 0.983. These results imply that the system's decoding performance can be made optimal by using quantum fluctuations.

2. Quantum Monte Carlo results

A d-dimensional quantum system can be transformed into a $(d+1)$-dimensional classical system by using the Trotter decomposition, as mentioned in Sec. IV. The local field at site x and the Trotter axis k can be written as

$$h_x(k) = -\frac{\beta}{2M}\sum_{i\neq x} J_{ix}\sigma_i(k) - \frac{B}{2}[\sigma_x(k-1)+\sigma_x(k+1)]. \tag{27}$$

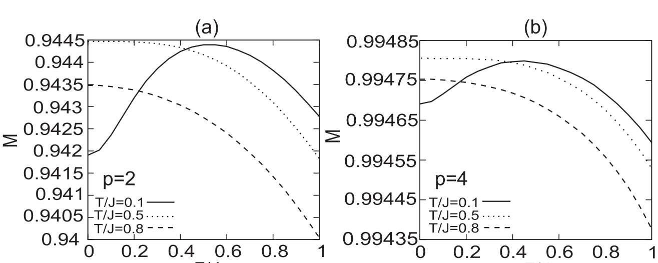

FIG. 4. Dependence of the overlap M on the level of quantum fluctuation Γ/J for $p=2$ (a) and $p=4$ (b) for $J_0/J=1.0$.

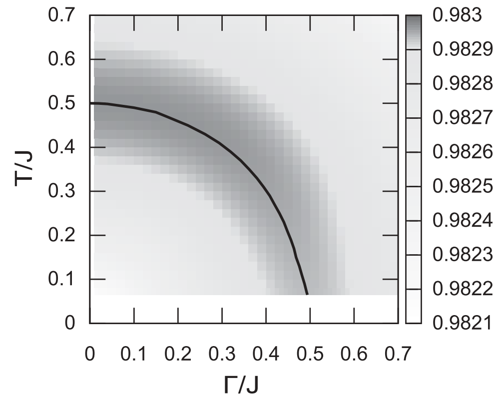

FIG. 5. Phase diagram for $p=3$ and $J_0/J=1.0$. The gradation represents the amount of the overlap. The solid line represents the maximal value of the overlap, i.e., $M\sim 0.983$.

In the METROPOLIS algorithm, the spin system is updated by the transition probability, $\mathrm{prob}[\sigma_x(k)=-\sigma_x(k)]=\exp(-\Delta H_{\mathrm{eff}})$ with $\Delta H_{\mathrm{eff}}=2h_x(k)\sigma_x(k)$ [27]. Accordingly, we can calculate the expectation $\langle\sigma_i\rangle$ and the overlap M under the ferromagnetic gauge.

Figures 6(a) and 6(b) plot the overlap M as a function of T/J in the cases of the classical system and $\Gamma/J=0.1$ for $p=2$, $N=500$, and $P=20$. We find that the overlap decreases in an overall sense. Figure 6(b) is a magnified view of Fig. 6(a), and the solid horizontal line is the maximum overlap obtained from the analysis. Here, we can see that each overlap is nonmonotonic and is a maximum at a finite temperature T/J. The decoding performance in the classical case is optimal at $T/J\sim 0.5$, which corresponds to the Nishimori

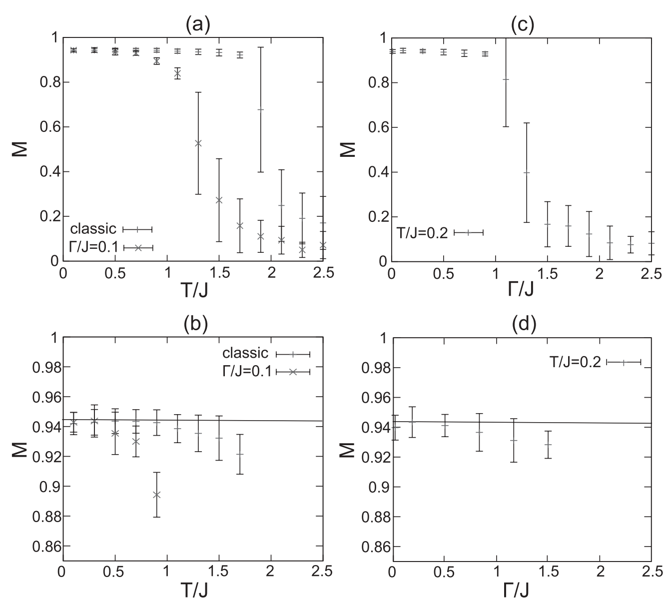

FIG. 6. (a) Dependence of overlap M on temperature T/J for $p=2$ and $J_0/J=1.0$. (b) Magnified view of (a). (c) Dependence of overlap M on quantum fluctuation Γ/J for $p=2$ and $J_0/J=1.0$. (d) Magnified view of (c). In (b) and (d), the horizontal line is the maximum value, 0.944, obtained by solving Eqs. (19)–(25) [see Fig. 4(a)]. The error bars in each figure were calculated by averaging over ten independent runs.

temperature. On the other hand, the optimal temperature shifts to the low-temperature region in the case of $\Gamma/J = 0.1$, but the maximum overlap, about 0.944, does not change. Figures 6(c) and 6(d) show the overlap M as a function of quantum fluctuation Γ/J. The overlap reaches a maximum (0.944) at finite Γ/J. These findings are qualitatively similar to the analytical results presented in the previous subsection.

3. Upper bound of the overlap

By theoretically estimating the upper bound of the overlap, we can show that the decoding performance in the presence of quantum fluctuations reaches the optimal performance for the classical system, $\Gamma = 0$.

To show this, we rewrite the overlap in the classical case defined by (9) as follows:

$$\begin{aligned}
M^{\text{classic}}(\beta) &= \mathop{\mathrm{Tr}}_{\xi} \int \prod_{i1<\cdots<ip} dJ_{i1,\ldots,ip} \frac{C_{Np}^{1/2}}{2^N} e^{f(J_{i1,\ldots,ip})} \exp\left(\beta_p \sum_{i1<\cdots<ip} J_{i1,\ldots,ip}\xi_{i1},\ldots,\xi_{ip}\right) \xi_i \mathrm{sgn}\left(\frac{\mathrm{Tr}\sigma_i e^{-\beta H}}{\mathrm{Tr}\, e^{-\beta H}}\right) \\
&\leqslant \int \prod_{i1<\cdots<ip} dJ_{i1,\ldots,ip} \frac{C_{Np}^{1/2}}{2^N} e^{f(J_{i1,\ldots,ip})} \left\| \mathop{\mathrm{Tr}}_{\xi} \xi_i \exp\left(\beta_p \sum_{i1<\cdots<ip} J_{i1,\ldots,ip}\xi_{i1},\ldots,\xi_{ip}\right)\right\| \left\| \mathrm{sgn}\left(\frac{\mathrm{Tr}\sigma_i e^{-\beta \hat{H}}}{\mathrm{Tr}\, e^{-\beta \hat{H}}}\right)\right\| \\
&\leqslant \int \prod_{i1<\cdots<ip} dJ_{i1,\ldots,ip} \frac{C_{Np}^{1/2}}{2^N} e^{f(J_{i1,\ldots,ip})} \left\| \mathop{\mathrm{Tr}}_{\xi} \xi_i \exp\left(\beta_p \sum_{i1<\cdots<ip} J_{i1,\ldots,ip}\xi_{i1},\ldots,\xi_{ip}\right)\right\| \equiv M_{\max}^{\text{classic}}.
\end{aligned} \tag{28}$$

Here, $C_{Np} = N^{p-1}/J^2\pi p!$, $f(J_{i1,\ldots,ip}) = -N^{p-1}J^2 p! \sum J_{i1,\ldots,ip}^2 - J_0 p!_N C_p/J^2 N^{p-1}$ for Eq. (1), and $M_{\max}^{\text{classic}}$ means the upper bound in the classical case. For the quantum system, the overlap (13) can be rewritten as follows:

$$\begin{aligned}
M(\beta,\Gamma) &= \mathop{\mathrm{Tr}}_{\xi} \int \prod_{i1<\cdots<ip} dJ_{i1,\ldots,ip} \frac{C_{Np}^{1/2}}{2^N} e^{f(J_{i1,\ldots,ip})} \exp\left(\beta_p \sum_{i1<\cdots<ip} J_{i1,\ldots,ip}\xi_{i1},\ldots,\xi_{ip}\right) \xi_i \mathrm{sgn}\left(\frac{\mathrm{Tr}\hat{\sigma}_i^z e^{-\beta \hat{H}}}{\mathrm{Tr}\, e^{-\beta \hat{H}}}\right) \\
&\leqslant \int \prod_{i1<\cdots<ip} dJ_{i1,\ldots,ip} \frac{C_{Np}^{1/2}}{2^N} e^{f(J_{i1,\ldots,ip})} \left\| \mathop{\mathrm{Tr}}_{\xi} \xi_i \exp\left(\beta_p \sum_{i1<\cdots<ip} J_{i1,\ldots,ip}\xi_{i1},\ldots,\xi_{ip}\right)\right\| \left\| \mathrm{sgn}\left(\frac{\mathrm{Tr}\hat{\sigma}_i^z e^{-\beta \hat{H}}}{\mathrm{Tr}\, e^{-\beta \hat{H}}}\right)\right\| \\
&\leqslant \int \prod_{i1<\cdots<ip} dJ_{i1,\ldots,ip} \frac{C_{Np}^{1/2}}{2^N} e^{f(J_{i1,\ldots,ip})} \left\| \mathop{\mathrm{Tr}}_{\xi} \xi_i \exp\left(\beta_p \sum_{i1<\cdots<ip} J_{i1,\ldots,ip}\xi_{i1},\ldots,\xi_{ip}\right)\right\| = M_{\max}^{\text{classic}}.
\end{aligned} \tag{29}$$

Thus, the optimal decoding performance in the presence of quantum fluctuations is the same as in the case of thermal fluctuation. Here, we can see that the maximum overlap of the classical system corresponds to the overlap at the Nishimori temperature $\beta_p = 2J_0/J^2$ for Eq. (28):

$$\begin{aligned}
M_{\max}^{\text{classic}} &= \int \prod_{i1<\cdots<ip} dJ_{i1,\ldots,ip} \frac{C_{Np}^{1/2}}{2^N} e^{f(J_{i1,\ldots,ip})} \frac{\left[\mathrm{Tr}_{\xi}\xi_i \exp\left(\beta_p \sum_{i1<\cdots<ip} J_{i1,\ldots,ip}\xi_{i1},\ldots,\xi_{ip}\right)\right]^2}{\left\|\mathrm{Tr}_{\xi}\xi_i \exp\left(\beta_p \sum_{i1<\cdots<ip} J_{i1,\ldots,ip}\xi_{i1},\ldots,\xi_{ip}\right)\right\|} \\
&= \mathop{\mathrm{Tr}}_{\xi} \int \prod_{i1<\cdots<ip} dJ_{i1,\ldots,ip} \frac{C_{Np}^{1/2}}{2^N} \exp\left\{-\frac{N^{p-1}}{J^2 N^{p-1}} \sum_{i1<\cdots<ip} \left(J_{i1,\ldots,ip} - \frac{J_0 p!}{N^{p-1}}\xi_{i1},\ldots,\xi_{i1}\right)^2\right\} \xi_i \\
&\quad \times \frac{\mathrm{Tr}_{\xi}\xi_i \exp\left(\beta_p \sum_{i1<\cdots<ip} J_{i1,\ldots,ip}\xi_{i1},\ldots,\xi_{ip}\right)}{\left\|\mathrm{Tr}_{\xi}\xi_i \exp\left(\beta_p \sum_{i1<\cdots<ip} J_{i1,\ldots,ip}\xi_{i1},\ldots,\xi_{ip}\right)\right\|} \\
&= \mathop{\mathrm{Tr}}_{\xi} \int \prod_{i1<\cdots<ip} dJ_{i1,\ldots,ip} \frac{C_{Np}^{1/2}}{2^N} \exp\left\{-\frac{N^{p-1}}{J^2 N^{p-1}} \sum_{i1<\cdots<ip} \left(J_{i1,\ldots,ip} - \frac{J_0 p!}{N^{p-1}}\xi_{i1},\ldots,\xi_{i1}\right)^2\right\} \xi_i \mathrm{sgn}\langle \xi_i \rangle_{\beta_p} \\
&= M(\beta_p).
\end{aligned} \tag{30}$$

The calculations in this section are similar to those presented in previous works [17,20].

VI. SUMMARY AND DISCUSSION

We discussed decoding the SOURLAS code in terms of a mean-field spin glass model with p-body interactions and quantum fluctuations introduced by means of a transverse field. First, we found that there is a phase transition from a ferromagnetic phase, which corresponds to an errorless phase, to a paramagnetic phase, which corresponds to a random guess phase, by solving the saddle-point equations derived by statistical mechanics. We also found that a spin glass phase occurs as the SN ratio decreases. Thus, we must appropriately control the quantum and thermal fluctuations in order to retrieve the original message.

Second, we evaluated the decoding performance in the presence of quantum fluctuations by solving the equation of the overlap between the original sequence and the decoded sequence derived from the equations of state for the order parameters. The MPM estimate incorporating quantum fluctuations seems to have roughly the same optimal performance as the thermal MPM estimate, i.e., finite-temperature decoding without quantum fluctuations. Thus, if we choose appropriate parameters for the quantum and thermal fluctuations, the decoding performance can be optimized, although it cannot exceed that of the thermal MPM estimate. A quantum Monte Carlo simulation with a finite number of spins was also carried out, and the results support the analysis.

Third, we found an upper bound for the overlap. The maximum overlap, which is a function of the thermal and quantum fluctuations, is that of the classical case. This means that the decoding performance with quantum fluctuations cannot exceed the classical case, but it can approach the optimal performance at the Nishimori temperature for the thermal MPM estimate. The analytical and simulation results contain this claim. Although the upper bound inequality does not clearly show that the MPM estimate based on the quantum fluctuation can achieve the same optimal performance as the thermal MPM estimate, it is nonetheless significant that the overlap has a (single) peak resulting in a maximum value at finite amplitude of the quantum fluctuation, even if we utilize numerical approaches instead of a mathematically rigorous argument to show this.

In obtaining our results, we used several approximations, including the replica symmetric approximation (RS) and the static approximation (SA). To clarify rigorously the properties of the error-correcting code described as the spin glass model, we will need to carefully check the validity of these approximations. The validity of the RS under SA could be checked by calculating the Almeida-Thouless (AT) line. The AT line has been analytically calculated for the SK model; however, the analysis was done under the SA only [14]. Ray *et al.* also attempted to draw the AT line by using Monte Carlo simulations, and they found that it might be possible to conclude that there is no replica symmetry breaking due to the quantum tunneling effects even in the low-temperature regime [29]. On the other hand, the validity of the SA has been shown in the case of the random energy model ($p \to \infty$) by using a large-p expansion. However, the SA may be invalid for the case of a finite p [24]. Hence, the limitation of the RS and SA is still an open question in the research field of spin glasses. Moreover, although we focused on the region of finite thermal and quantum fluctuation in this paper, the decoding performance of a pure quantum system that has no thermal fluctuation remains an open question. An analytical treatment of this question will require one to derive the equations of state for the order parameters and the overlap in the low-temperature limit.

ACKNOWLEDGMENTS

This work was partially supported by Grants-in-Aid for Scientific Research (No. 90233345, No. 20240020, and No. 22700230) and for Japan Society for the Promotion of Science (JSPS) Fellows (No. 12J06501) from the Ministry of Education, Culture, Sports, Science and Technology of Japan. One of the authors (J.I.) was financially supported by a Grant-in-Aid for Scientific Research (B) of Japan Society for the Promotion of Science, No. 80217017.

APPENDIX: DERIVATION OF THE OVERLAP

Here, we derive the expression for the overlap M (25) in a similar way to the classical case [26]. Adding $h\sum_i \sigma_i^\mu(t)\sigma_i^\nu(t')$ to the partition function $[Z^n]$, we obtain

$$[Z^n] = \frac{1}{2^N}\operatorname*{Tr}_{\boldsymbol{\xi}}\int\prod_{i_i<\cdots<i_p} dJ_{i_1,\ldots,i_p}\left(\frac{N^{p-1}}{\pi J^2 p!}\right)^{\frac{1}{2}}\exp\left\{-\frac{N^{p-1}}{J^2 p!}\sum_{i_1<\cdots<i_p}\left(J_{i_1,\ldots,i_p}-\frac{J_0 p!}{N^{p-1}}\xi_{i_1},\ldots,\xi_{i_p}\right)^2\right\}$$
$$\times\operatorname*{Tr}_{\boldsymbol{\sigma}}\exp\left(\frac{\beta}{P}\sum_\mu\sum_{i_i<\cdots<i_p}\sum_t J_{i_1,\ldots,i_p}\sigma_{i_1}^\mu(t),\ldots,\sigma_{i_p}^\mu(t)+B\sum_\mu\sum_i\sum_t\sigma_i^\mu(t)\sigma_i^\mu(t+1)+h\sum_i\sigma_i^\mu(t)\sigma_i^\nu(t')\right), \quad \text{(A1)}$$

where $B=\log(\coth\frac{\beta\Gamma}{P})/2$, and $\boldsymbol{\sigma}=(\boldsymbol{\sigma}^1,\ldots,\boldsymbol{\sigma}^n),\boldsymbol{\sigma}^k=[\sigma_1^k(t),\ldots,\sigma_N^k(t)]$, $t=1,\ldots,P$ from Eqs. (1) and (17). The expression μ and ν represent the replica indices and t represents the Trotter index. Applying a gauge transformation

$$\sigma_i\to\sigma_i\xi_i,\quad J_{i_1,\ldots,i_p}\to J_{i_1,\ldots,i_p}\xi_{i1},\ldots,\xi_{ip} \quad \text{(A2)}$$

to Eq. (A1) removes $\boldsymbol{\xi}$ from the integrand. The problem is equivalent to the case of $\xi_i=1$ $(\forall i)$, i.e., the ferromagnetic gauge. Thus, we can carry out the Gaussian integration in Eq. (A1), in which the form of $[Z^n]$ is written as

$$[Z^n] = \mathop{\mathrm{Tr}}_{\sigma} \exp\left\{B\sum_{i,t,\mu}\sigma_i^\mu(t)\sigma_i^\mu(t+1) + h\sum_i \sigma_i^\mu(t)\sigma_i^\nu(t') + \frac{\beta^2 J^2 N}{4P^2}\sum_{t,t'}\sum_{\mu,\nu}\left(\frac{1}{N}\sum_i \sigma_i^\mu(t)\sigma_i^\nu(t')\right)^p + \frac{J_0 N\beta}{P}\sum_{t,\mu}\left(\frac{1}{N}\sum_i \sigma_i^\mu(t)\right)^p\right\}. \tag{A3}$$

Let us rewrite (A3) in terms of new variables,

$$m_\mu(t) = \frac{1}{N}\sum_i \sigma_i^\mu(t), \tag{A4}$$

$$Q_{\mu\nu}(t,t') = \frac{1}{N}\sum_i \sigma_i^\mu(t)\sigma_i^\nu(t'), \tag{A5}$$

$$Q_{\mu\mu}(t,t') = \frac{1}{N}\sum_i \sigma_i^\mu(t)\sigma_i^\mu(t'). \tag{A6}$$

Now we can evaluate the integral in the thermodynamic limit $N \to \infty$, and we rewrite the partition function as

$$[Z^n] \simeq F_n(m_\mu(t),\hat{m}_\mu(t),Q_{\mu\mu}(t),\hat{Q}_{\mu\mu}(t),Q_{\mu\nu}(t),\hat{Q}_{\mu\nu}(t)) = \exp(-\beta nNf), \tag{A7}$$

$$-\beta nf = \sum_{t,\mu}\left(\frac{J_0\beta}{P}m_\mu(t)^p - \frac{1}{P}\hat{m}_\mu(t)m_\mu(t)\right) + \sum_{t,t',\mu}\left(\frac{\beta^2 J^2}{4P^2}Q_{\mu\mu}(t,t')^p - \frac{1}{P^2}\hat{Q}_{\mu\mu}(t,t')Q_{\mu\mu}(t,t')\right) + \sum_{t,t',\mu<\nu}\left(\frac{\beta^2 J^2}{2P^2}Q_{\mu\nu}(t,t')^p - \frac{1}{P^2}\hat{Q}_{\mu\nu}(t,t')Q_{\mu\nu}(t,t')\right) + \log \mathop{\mathrm{Tr}}_{\sigma} e^L, \tag{A8}$$

$$L = \frac{1}{P}\sum_{t,\mu}\hat{m}_\mu(t)\sigma^\mu(t) + \frac{1}{P^2}\sum_{t,t',\mu}\hat{Q}_{\mu\mu}(t,t')\sigma^\mu(t) + \frac{1}{P^2}\sum_{t,t',\mu<\nu}\hat{Q}_{\mu\nu}(t,t')\sigma^\mu(t)\sigma^\nu(t) + B\sum_{t,\mu}\sigma^\mu(t)\sigma^\mu(t+1) + h\sigma^\mu(t)\sigma^\nu(t'), \tag{A9}$$

where $(\hat{\cdot})$ means the Fourier-transformed expressions. The above equations contain an additional field $h\sigma^\mu(t)\sigma^\nu(t')$, which is a simple extension of previous research [24,28].

We differentiate $-\beta nf$ with respect to h, as follows:

$$\frac{\partial(-\beta nf)}{\partial h} = \frac{\mathrm{Tr}_{\sigma}\sigma^\mu(t)\sigma^\nu(t')e^L}{\mathrm{Tr}_{\sigma}\, e^L}, \tag{A10}$$

where we see that $\sigma^\mu(t')\sigma^\nu(t')$ is outside the exponent e^L. Our goal is to calculate Eq. (A10) in the limit of $n \to 0$, $h \to 0$ and to prove the expression (25) in the same sense as in the previous study [26].

The replica symmetry (RS) and static approximation (SA) lead to

$$\sum_\mu\sum_{t,t'}\sigma^\mu(t)\sigma^\mu(t') = \sum_\mu\left(\sum_t \sigma^\mu(t)\right)^2, \tag{A11}$$

$$\sum_{\mu<\nu}\sum_{t,t'}\sigma^\mu(t)\sigma^\nu(t') = \frac{1}{2}\left\{\left(\sum_\mu\sum_{t,t'}\sigma^\mu(t)\right)^2 - \sum_\mu\left(\sum_t \sigma^\mu(t)\right)^2\right\}. \tag{A12}$$

By using the Hubbard-Stratonovich transformation,

$$\exp\left(\frac{x^2}{2}\right) = \int\frac{dz}{\sqrt{2}}\exp\left(-\frac{z^2}{2}+xz\right) = \int Dz\exp(xz), \quad \left(Dz \equiv \frac{dz}{\sqrt{2\pi}}\right), \tag{A13}$$

we can calculate the exponent in Eq. (A8) as follows:

$$e^L = \exp\left(\frac{\hat{m}}{P}\sum_{t,\mu}\sigma^\mu(t) + B\sum_{t,\mu}\sigma^\mu(t)\sigma^\mu(t+1) + \sigma^\mu(t')\sigma^\nu(t)\right) \times \int Dw\exp\left(\frac{\sqrt{\hat{q}}}{P}\sum_{t,\alpha}\sigma^\mu(t)w\right)\prod_\mu\int Dz\exp\left(\frac{\sqrt{2\hat{\chi}-\hat{q}}}{P}\sum_t \sigma^\mu(t)z\right)$$

$$= \int Dw \prod_{\gamma\neq\mu,\nu} \int Dz \exp\left(B\sum_t \sigma^\gamma(t)\sigma^\gamma(t+1) + \frac{\hat{m}+\sqrt{\hat{q}}w+\sqrt{2\hat{\chi}-\hat{q}}z}{P}\sum_t \sigma^\gamma(t)\right)$$
$$\times \int Dz \exp\left(B\sum_{t,\gamma=\mu,\nu} \sigma^\gamma(t)\sigma^\gamma(t+1) + \frac{\hat{m}+\sqrt{\hat{q}}w+\sqrt{2\hat{\chi}-\hat{q}}z}{P}\sum_{t,\gamma=\mu,\nu} \sigma^\gamma(t) + h\sigma^\mu(t)\sigma^\nu(t')\right). \tag{A14}$$

Using the Trotter formula, we can take the spin trace in the limit $P\to\infty$ as

$$\mathop{\mathrm{Tr}}_{\sigma}\exp\left(B\sum_t \sigma^\mu(t)\sigma^\mu(t+1) + \frac{\Phi}{P}\sum_t \sigma^\mu(t)\right) = \mathop{\mathrm{Tr}}_{\sigma}\exp(\Gamma\hat{\sigma}^x + \Phi\hat{\sigma}^z)$$
$$= 2\cosh\sqrt{\Phi^2+\Gamma^2}$$
$$= 2\cosh\Xi, \tag{A15}$$

where $\Phi/\beta = \hat{m}+\sqrt{\hat{q}}w+\sqrt{2\hat{\chi}-\hat{q}}z$ and $\Xi \equiv \sqrt{\Phi^2+\beta^2\Gamma^2}$. Therefore, we obtain the final form of $\mathrm{Tr}_{\boldsymbol{\sigma}}\, e^L$ and $\mathrm{Tr}_{\boldsymbol{\sigma}}\sigma^\mu(t)\sigma^\nu(t')e^L$ in the limit $h\to 0$, respectively. The results are given by

$$\mathop{\mathrm{Tr}}_{\sigma} e^L = \int Dw\left(\int Dz\ \cosh\Xi\right)^n, \tag{A16}$$

$$\mathop{\mathrm{Tr}}_{\sigma}\sigma^\mu(t)\sigma^\nu(t)\ e^L = \int Dw\left(\int Dz\ 2\cosh\Xi\right)^{n-2}\mathop{\mathrm{Tr}}_{\boldsymbol{\sigma}^\mu}\int Dz\,\sigma^\mu(t)\exp\left(B\sum_t \sigma^\mu(t)\sigma^\mu(t+1)+\frac{\Phi}{P}\sum_t\sigma^\mu(t)\right)$$
$$\times \mathop{\mathrm{Tr}}_{\boldsymbol{\sigma}^\nu}\int Dz\,\sigma^\nu(t)\exp\left(B\sum_t \sigma^\nu(t)\sigma^\nu(t+1)+\frac{\Phi}{P}\sum_t\sigma^\nu(t)\right). \tag{A17}$$

Equation (A16) corresponds to the denominator of Eq. (A10), which is equal to 1 in the limit of $n\to 0$.

To calculate the right-hand side of Eq. (A17), we differentiate both sides of the Trotter formula (A15) with respect to Φ. Then we have

$$\mathop{\mathrm{Tr}}_{\sigma}\frac{1}{P}\sum_t \sigma^\mu(t)\exp\left(B\sum_t \sigma^\mu(t)\sigma^\mu(t+1)+\frac{\Phi}{P}\sum_t\sigma^\mu(t)\right) = \frac{2\Phi}{\sqrt{\Phi^2+\Gamma^2}}\sinh\sqrt{\Phi^2+\Gamma^2}. \tag{A18}$$

Thus, we obtain the following equation:

$$\mathop{\mathrm{Tr}}_{\sigma}\sigma^\mu(t)\sigma^\nu(t)\ e^L = \int Dw\left(\int Dz\ 2\cosh\Xi\right)^n \frac{\left(\int Dz\ \frac{\Phi}{\Xi}2\sinh\Xi\right)^2}{\left(\int Dz\ 2\cosh\Xi\right)^2} \to \int Dw\left(\frac{\int Dz\ \frac{\Phi}{\Xi}\sinh\Xi}{\int Dz\ \cosh\Xi}\right)^2 \quad (n\to 0) \tag{A19}$$

for

$$\mathop{\mathrm{Tr}}_{\boldsymbol{\sigma}^\nu}\int Dz\,\sigma^\nu(t)\exp\left(B\sum_t \sigma^\nu(t)\sigma^\nu(t+1)+\frac{\Phi}{P}\sum_t\sigma^\nu(t)\right) = \int Dz\ \frac{\Phi}{\Xi}2\sinh\Xi \tag{A20}$$

under the RS and SA. We can extend the above methods to the case of an external field with the product of k spins, $h\sum_i \sigma_i^\mu(t)\sigma_i^\nu(t'),\ldots$. In such a case, we get

$$\left[\langle\sigma\rangle_{\beta,\Gamma}^k\right] = \int Dw\left(\frac{\int Dz\ \frac{\Phi}{\Xi}\sinh\Xi}{\int Dz\ \cosh\Xi}\right)^k. \tag{A21}$$

For an arbitrary function $F(x)$ that can be expanded around $x=0$, the above equation can be expanded to

$$[F(\langle\sigma\rangle_{\beta,\Gamma})] = \int Dw\ F\left(\frac{\int Dz\ \frac{\Phi}{\Xi}\sinh\Xi}{\int Dz\ \cosh\Xi}\right). \tag{A22}$$

If we take $F(x)$ to be a function $\mathrm{sgn}(x)$ [e.g., $\tanh(ax)$ with $a\to\infty$], we obtain the overlap M in the form

$$M(\beta,\Gamma) = [\mathrm{sgn}(\langle\sigma\rangle_{\beta,\Gamma})] = \int Dw\ \mathrm{sgn}\left(\frac{\int Dz\ \frac{\Phi}{\Xi}\sinh\Xi}{\int Dz\ \cosh\Xi}\right). \tag{A23}$$

[1] K. Tanaka, J. Phys. A **35**, 81 (2002).
[2] N. Sourlas, Nature (London) **339**, 693 (1989).
[3] J. J. Hopfield, Proc. Natl. Acad. Sci. (USA) **79**, 2554 (1982).
[4] J. Inoue, J. Phys. A **30**, 1047 (1997).
[5] D. C. Mattis, Phys. Lett. A **56**, 421 (1976).
[6] P. Rujan, Phys. Rev. Lett. **70**, 2968 (1993).
[7] Y. Kabashima and D. Saad, Europhys. Lett. **45**, 98 (1999).
[8] A. Montanari and N. Sourlas, Eur. Phys. J. B **18**, 121 (2000).
[9] B. K. Chakrabarti, A. Dutta, and P. Sen, *Quantum Ising Phases and Transitions in Transverse Ising Models* (Springer, Berlin, 1996).
[10] H. Ishii and T. Yamamoto, J. Phys. C **18**, 6225 (1985).
[11] D. Thirumalai, Q. Li, and T. R. Kirkpatrick, J. Phys. A **22**, 3339 (1989).
[12] Y. Y. Goldschmidt, Phys. Rev. B **41**, 4858 (1990).
[13] Y. Y. Goldschmidt and P.-Y. Lai, Phys. Rev. Lett. **64**, 2467 (1990).
[14] D.-H. Kim and J.-J. Kim, Phys. Rev. B **66**, 054432 (2002).
[15] E. Farhi, J. Goldstone, S. Gutmann, J. Lapan, A. Lundgren, and D. Preda, Science **292**, 472 (2001).
[16] R. Martonak, G. E. Santoro, and E. Tosatti, Phys. Rev. E **70**, 057701 (2004).
[17] J. I. Inoue, Phys. Rev. E **63**, 046114 (2001).
[18] D. Sherrington and S. Kirkpatrick, Phys. Rev. Lett. **35**, 1792 (1975).
[19] B. Derrida, Phys. Rev. B **24**, 2613 (1981).
[20] H. Nishimori and K. Y. M. Wong, Phys. Rev. E **60**, 132 (1999).
[21] J. Inoue, Y. Saika, and M. Okada, J. Conf. Ser. **143**, 012019 (2009).
[22] A. B. Finnila, M. A. Gomez, C. Sebenik, C. Stenson, and J. D. Doll, Chem. Phys. Lett. **219**, 343 (1994).
[23] M. Suzuki, Prog. Theor. Phys. **56**, 1454 (1976).
[24] T. Obuchi, H. Nishimori, and D. Sherrington, J. Phys. Soc. Jpn. **76**, 054002 (2007).
[25] A. J. Bray and M. A. Moore, J. Phys. C **13**, L665 (1980).
[26] H. Nishimori, *Statistical Physics of Spin Glasses and Information Processing* (Oxford Science Publications, Oxford, 2001).
[27] N. Metropolis, A. W. Rosenbluth, M. N. Rosenbluth, A. H. Teller, and E. Teller, J. Chem. Phys. **21**, 1087 (1953).
[28] J. Inoue, *Quantum Spin Glasses, Quantum Annealing and Probabilistic Information Processing*, Lecture Notes in Physics, Vol. 679 (Springer, Berlin, 2005), p. 259.
[29] P. Ray, B. K. Chakrabarti, and A. Chakrabarti, Phys. Rev. B **39**, 11828 (1989).